

Selective determination of trace boron based on resonance Rayleigh scattering energy transfer from nanogold aggregate to complex of boric acid-azomethine-H

Lingling Ye^a, Guiqing Wen^a, Yanghe Luo^{a,b}, Hua Deng^a, Lening Hu^a, Caiyan Kang^a, Fanggui

Ye^a, Aihui Liang^{*a}, Zhiliang Jiang^{*a}

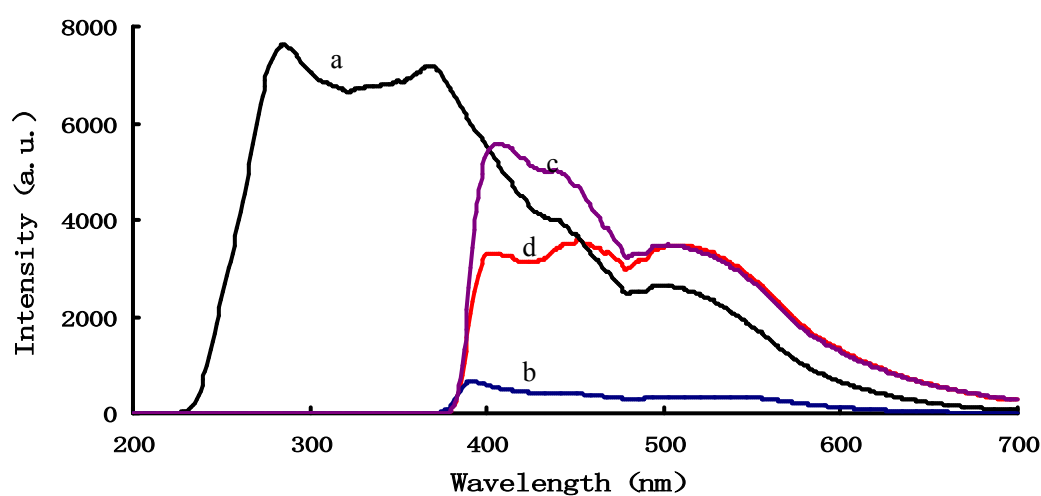


Figure 1S RRS spectra of the AMH-AuNPs-boron system

(a) 200 ng/ml B-0.17 μ g/ml AuNPs -pH 5.6 NH₄AC-HAc; (b) 200 ng/ml B-0.17 μ g/ml AuNPs-7.5 $\times 10^{-4}$ g/ml azomethine -H; (c) pH 5.6 NH₄AC-HAc -7.5 $\times 10^{-4}$ g/ml AMH -0.17 μ g/ml AuNPs; (d) pH 5.6 NH₄AC-HAc -7.5 $\times 10^{-4}$ g/ml AMH-0.17 μ g/ml AuNPs-200 ng/ml B.

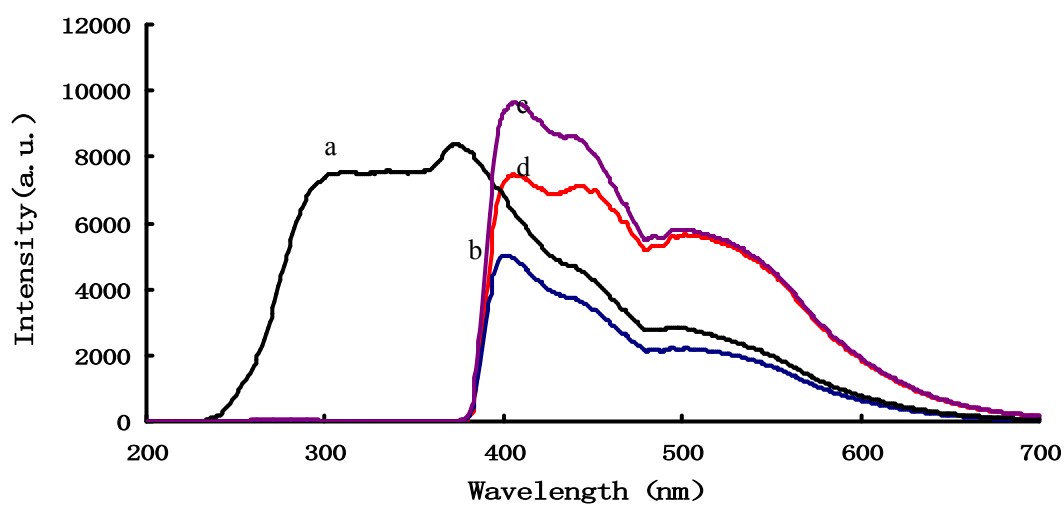


Figure 2S RRS spectra of the AMH-HAuCl₄-boron system

(a) 200 ng/mL B-pH 5.6 NH₄AC-HAc -0.375μg/ml HAuCl₄; (b) 200 ng/mL B- 7.5×10⁻⁴g/ml AMH - 0.375μg/ml HAuCl₄; (c) pH 5.6 NH₄AC-HAc -7.5×10⁻⁴g/ml AMH -0.375μg/ml HAuCl₄; (c) pH 5.6 NH₄AC-HAc -7.5×10⁻⁴g/ml AMH- -0.375μg/ml HAuCl₄-200 ng/mL B.

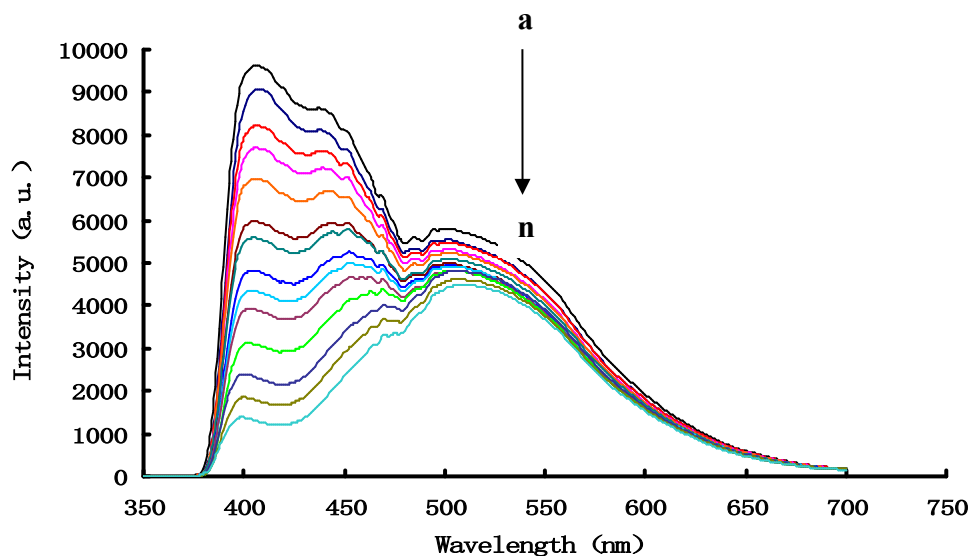


Figure 3S RRS spectra of the B-AMH-HAuCl₄ system

(a) 2.5×10⁻²g/ml pH 5.6 NH₄AC-HAc -7.5×10⁻⁴g/ml AMH -0.375μg/ml HAuCl₄; (b) a+5 ng/ml B; (c) a+40 ng/ml B; (d) a+80 ng/ml B; (e) a+100 ng/ml B; (f) a+150 ng/ml B; (g) a+200 ng/ml B; (h) a+250 ng/ml B; (i) a+300 ng/ml B; (j) a+350 ng/ml B; (k) a+400 ng/ml B; (l) a+450 ng/ml B; (m) a+500 ng/ml B; (n) a+600 ng/ml B.

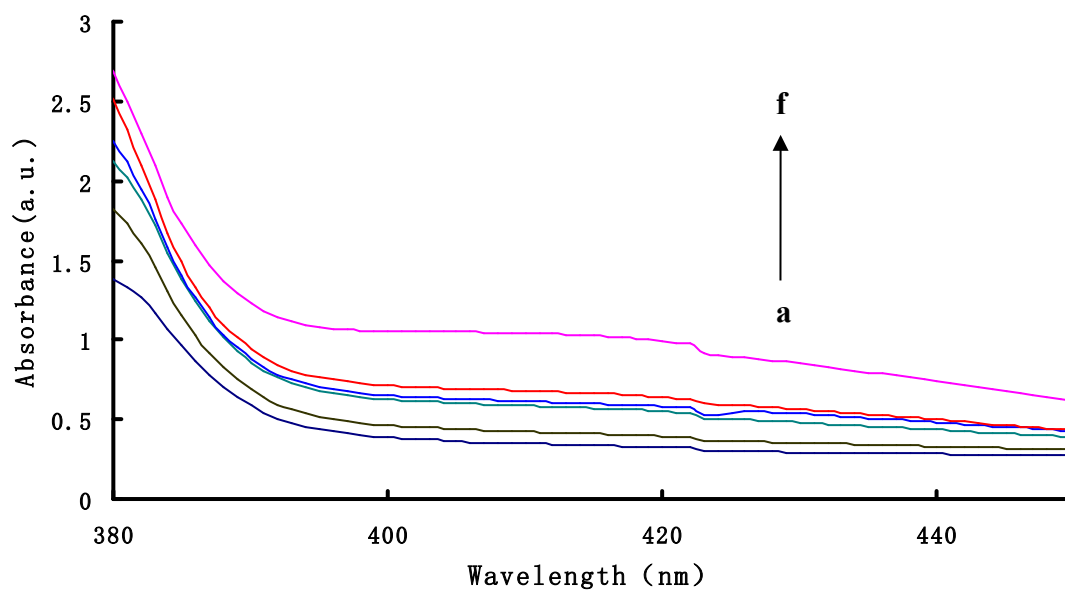


Figure 4SA Absorption spectra of the B-AMH-AuNP system

(a) pH 5.6 $\text{NH}_4\text{Ac-HAc}$ $-7.5 \times 10^{-4} \text{g/mL}$ AMH- $0.17 \mu\text{g/mL}$ AuNPs; (b) a+100 ng/mL B; (c) a+200 ng/mL B; (d) a+250 ng/mL B; (e) a+600 ng/mL B; (f) a+650 ng/mL B.

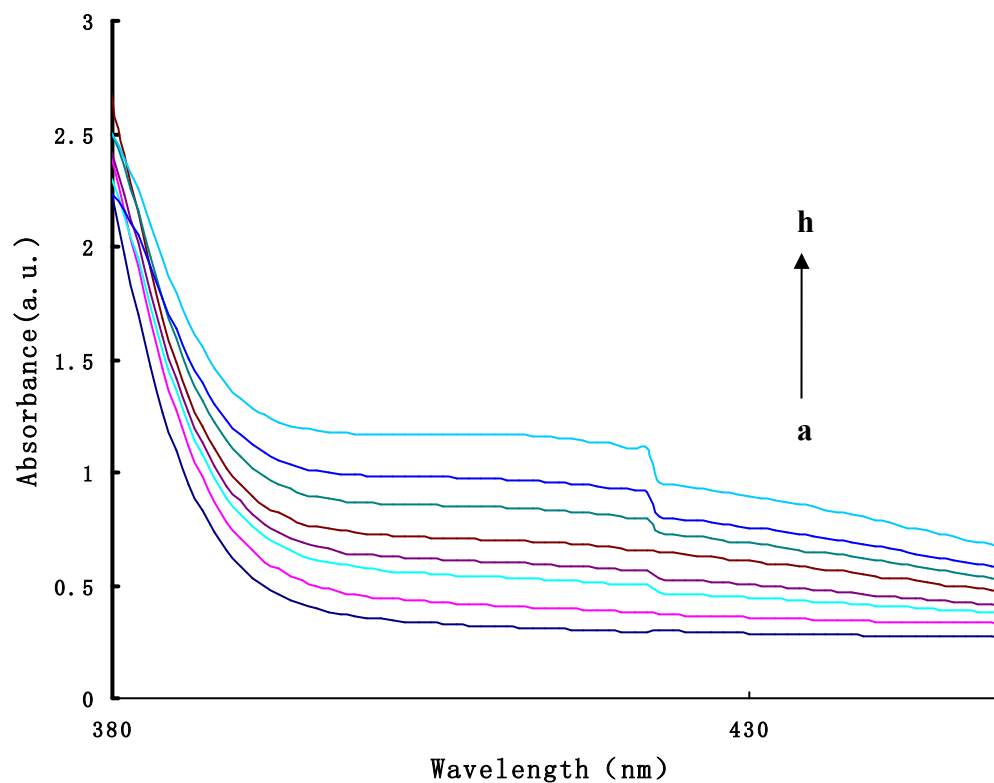


Figure 4SB Absorption spectra of the B-AMH- HAuCl_4 system

(a) pH 5.6 $\text{NH}_4\text{AC-HAc}$ $-7.5 \times 10^{-4} \text{g/mL}$ AMH $-0.375 \mu\text{g/mL}$ HAuCl_4 ; (b) a+50 ng/mL B; (c) a+75 ng/mL B; (d) a+200 ng/mL B; (e) a+300 ng/mL B; (f) a+400 ng/ml B; (g) a+600 ng/mL B; (h) a+7500 ng/mL B.

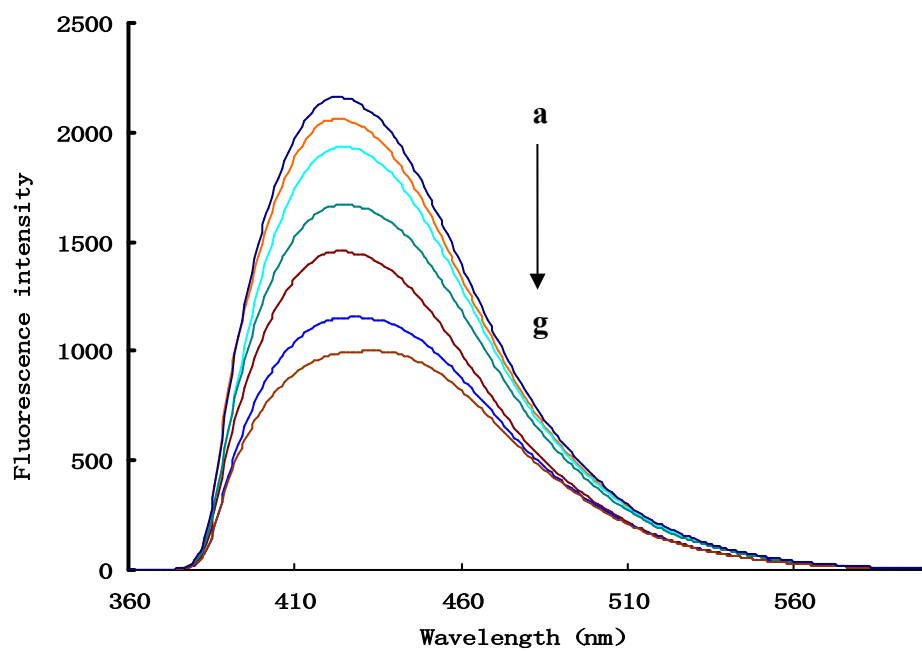


Figure 5S Fluorescence spectra of the B-AMH system

(a) 2.5×10^{-2} g/ml pH 5.6 $\text{NH}_4\text{AC-HAc}$ - 7.5×10^{-4} g/ml AMH; (b) a+10 ng/ml B; (c) a+25 ng/ml B; (d) a+100 ng/ml B; (e) a+200 ng/ml B; (f) a+240 ng/ml B; (g) a+300 ng/ml B.

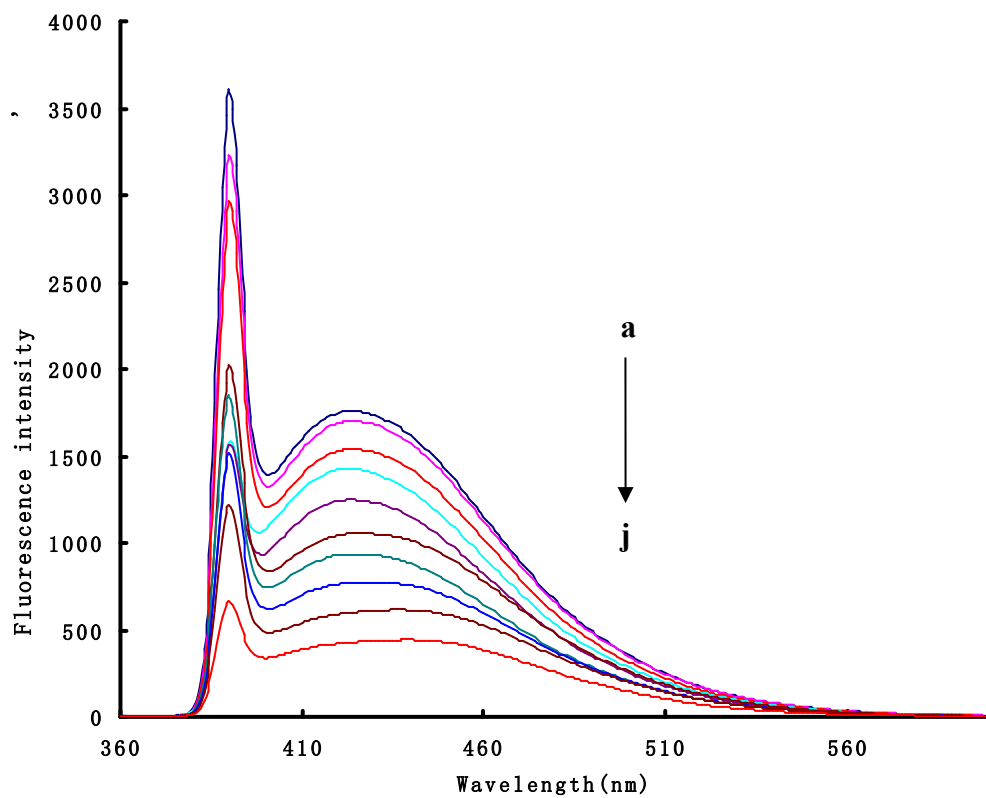


Figure 6S Fluorescence spectra of the B-AMH-HAuCl₄ system

(a) 0.375 μg/ml HAuCl₄-2.5 × 10⁻²g/ml pH 5.6 NH₄AC-HAc -7.5 × 10⁻⁴g/ml AMH; (b) a+1 ng/ml B; (c) a+2.5 ng/ml B; (d) a+5 ng/ml B; (e) a+50 ng/ml B; (f) a+100 ng/ml B; (g) a+200 ng/ml B; (h) a+300 ng/ml B; (i) a+400 ng/ml B; (j) a+500 ng/ml B.

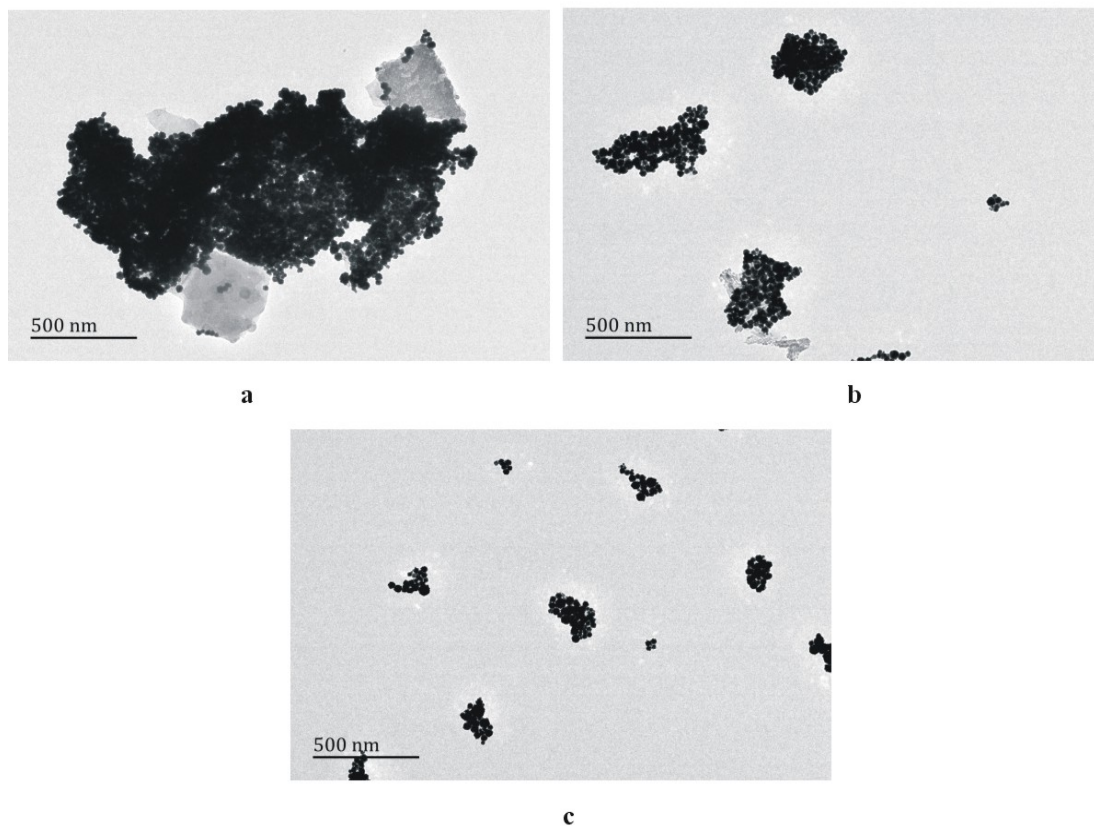
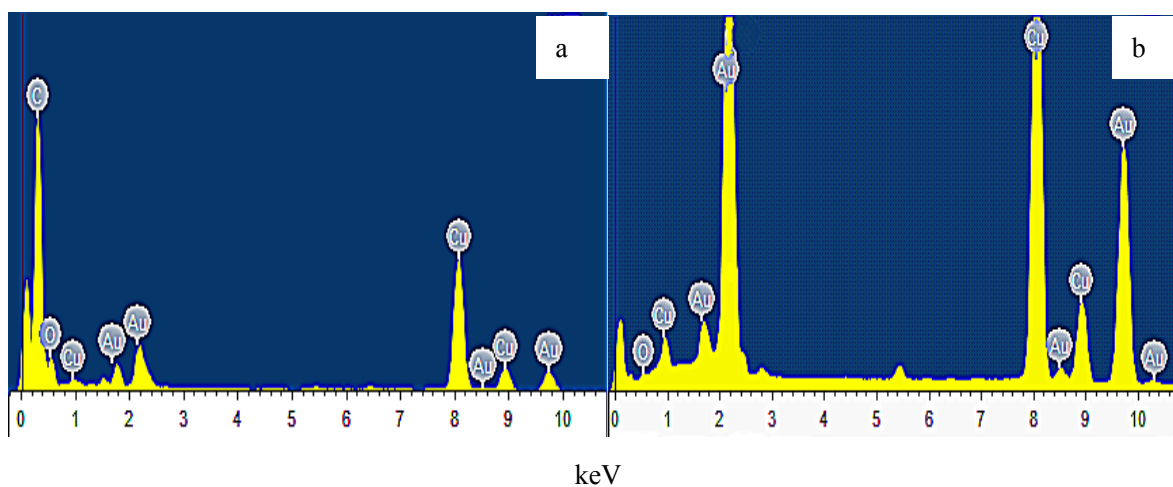


Figure 7S TEM of the boron-AMH- AuNPs system

a: pH 5.6 NH₄AC-HAc -7.5 × 10⁻⁴g/ml AMH-0.375 μg/ml HAuCl₄; b: a+250 ng/ml H₃BO₃; c: a+500 ng/ml H₃BO₃.



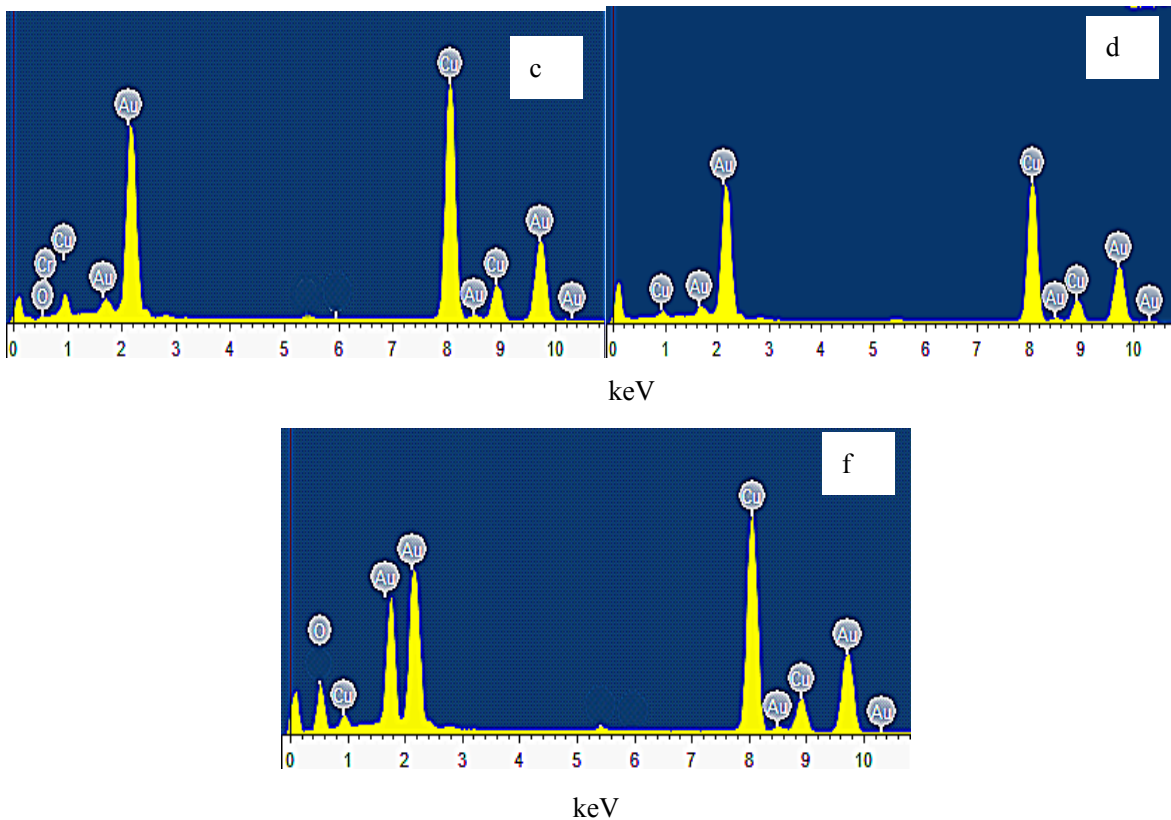


Figure 8S Energy spectra of the boron-AMH- AuNPs system

a: 0.17 μ g/ml AuNPs; b: pH 5.6 NH₄AC-HAc -7.5 $\times 10^{-4}$ g/ml AMH -0.17 μ g/ml AuNPs; c: b+500ng/ml B;
 d: pH 5.6 NH₄AC-HAc-7.5 $\times 10^{-4}$ g/ml AMH -0.375 μ g/ml HAuCl₄; e: d+500ng/ml B.

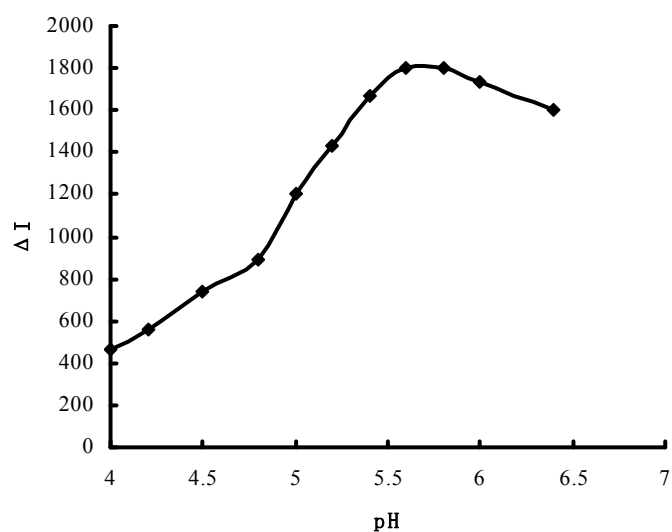


Figure 9S Effect of pH of buffer solution

200 ng/ml B -2.5 $\times 10^{-2}$ g/ml NH₄AC-HAc -7.5 $\times 10^{-4}$ g/ml AMH -0.17 μ g/ml AuNPs

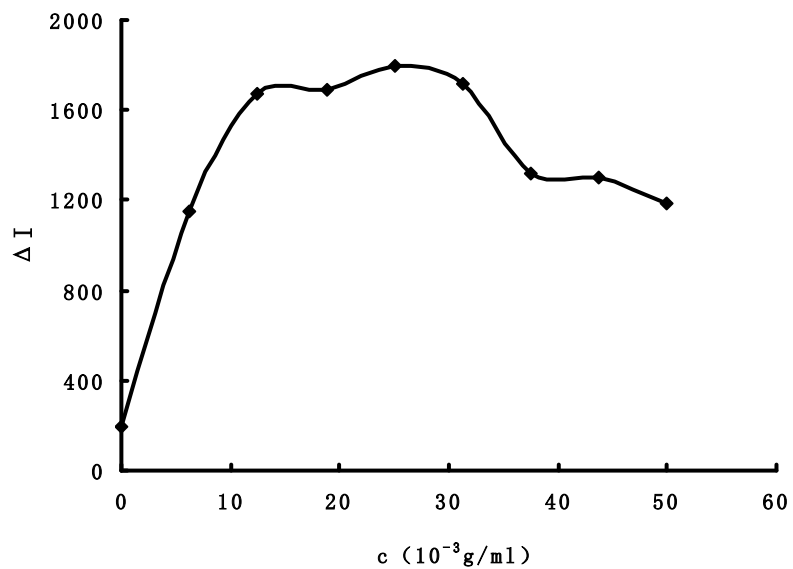


Figure 10S Effect of concentration of buffer solution

200 ng/ml B-pH 5.6 NH₄AC-HAc -7.5×10⁻⁴g/ml AMH -0.17μg/ml AuNPs

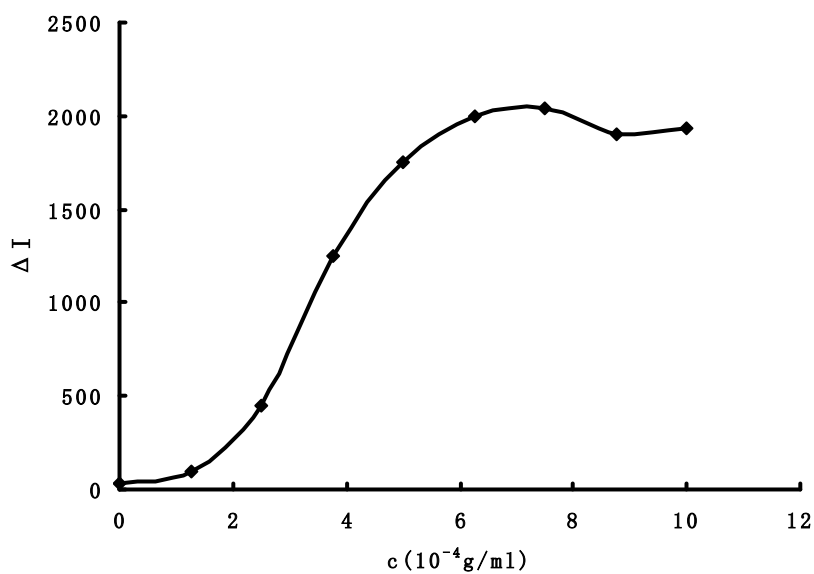


Figure 11S Effect of AMH concentration

200 ng/ml B -2.5×10⁻²g/ml pH 5.6 NH₄AC-HAc - AMH -0.17μg/ml AuNPs;

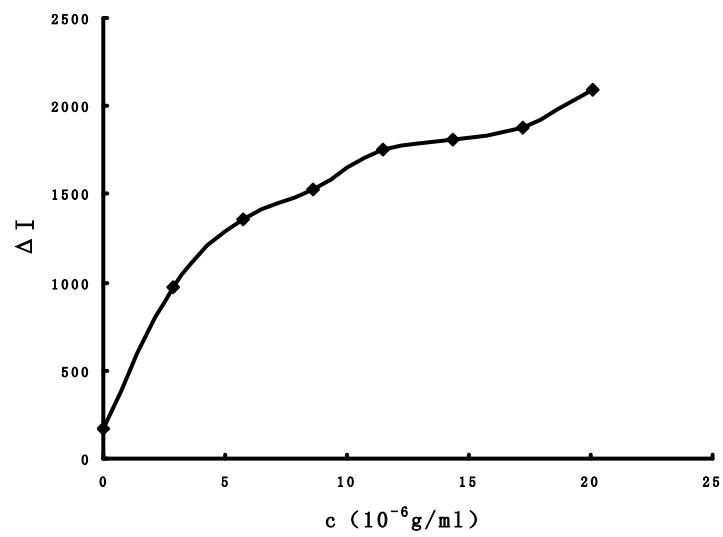


Figure 12S Effect of AuNPs- concentration
 200 ng/mlB-pH 5.6 NH₄AC-HAc -7.5×10⁻⁴g/ml AMH - AuNPs

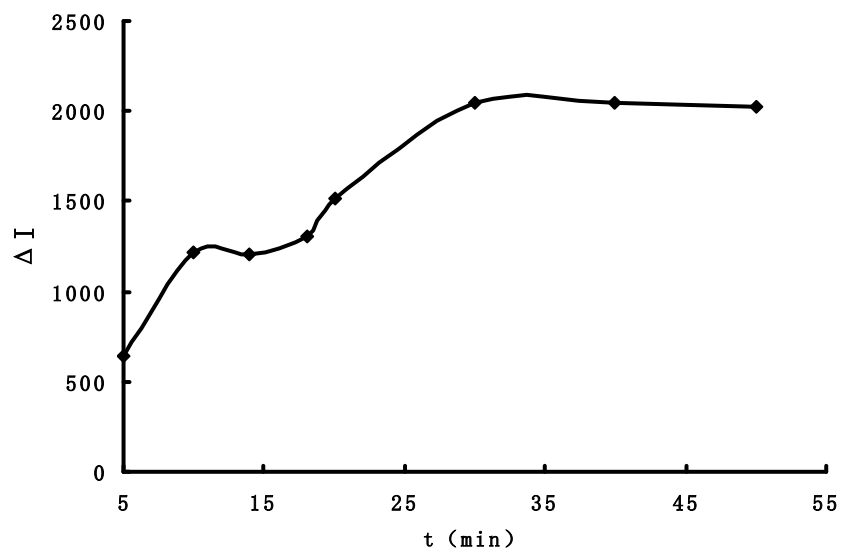


Figure 13S Effect of AMH and boron reaction time
 200 ng/mlB -pH 5.6 NH₄AC-HAc -7.5×10⁻⁴g/ml AMH -0.17μg/ml AuNPs

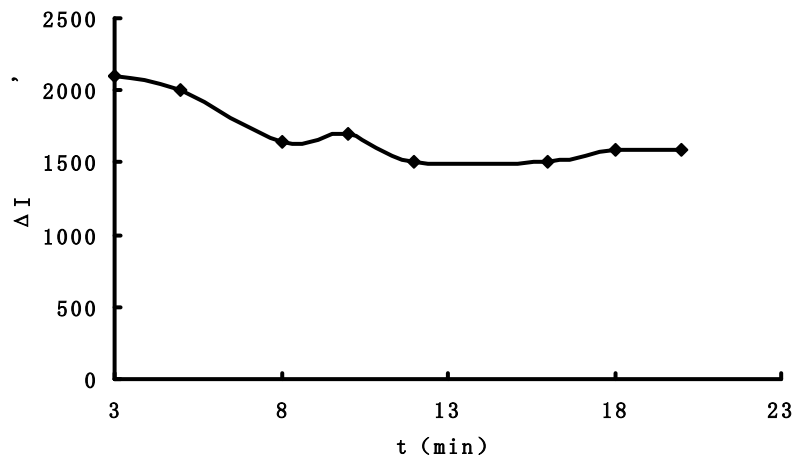


Figure 14S Effect of the time complexes react with AuNPs
 200 ng/mlB -pH 5.6 NH₄AC-HAc -7.5×10⁻⁴g/ml AMH -0.17μg/ml AuNPs

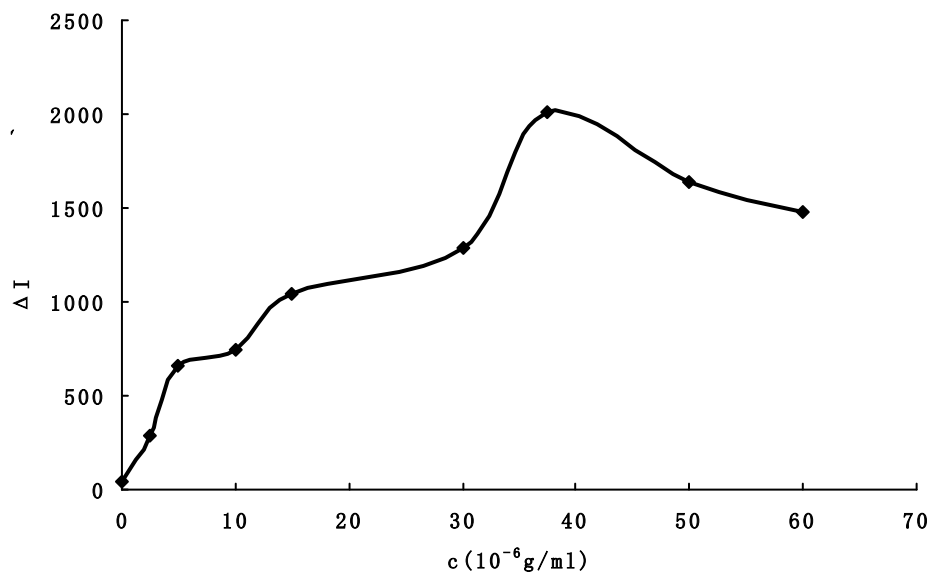


Figure 15S Effect of HAuCl₄ concentration
 200 ng/mlB - pH 5.6 NH₄AC-HAc -7.5×10⁻⁴g/ml AMH

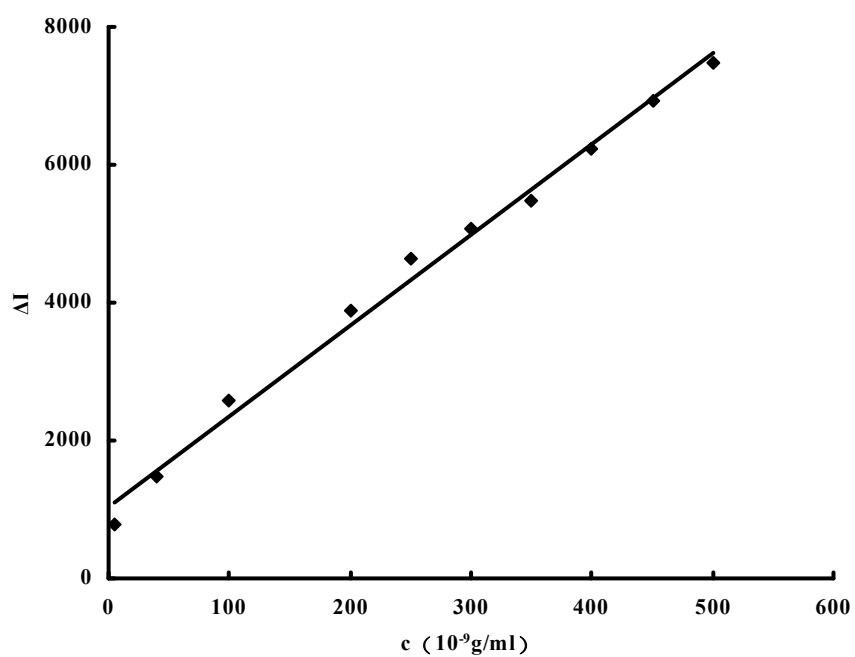


Fig. 16S Working curve of the boron-AMH- AuNPs Rayleigh scattering system
 pH 5.6 NH₄AC-HAc -7.5×10⁻⁴g/ml AMH -0.375μg/mL HAuCl₄

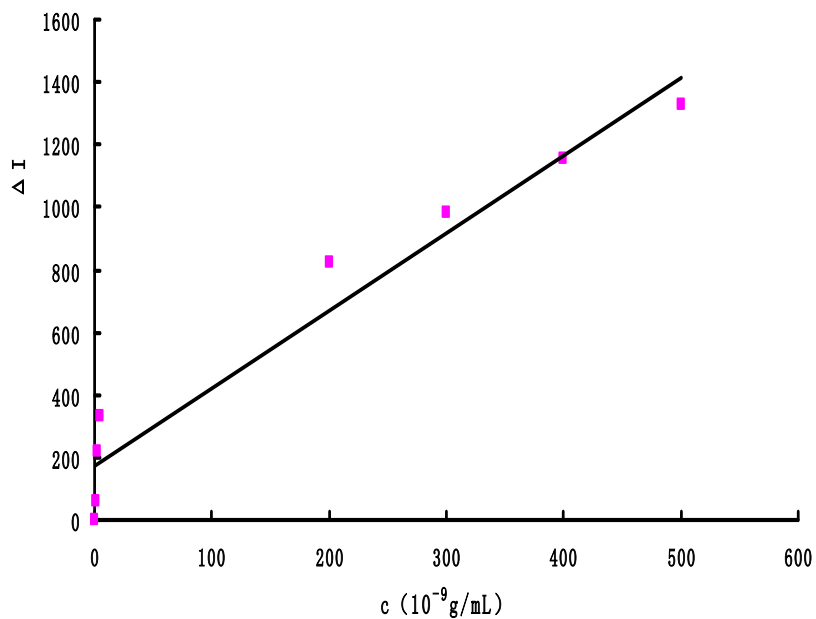


Fig. 17S curve of AMH- AuNPs-boron fluorescence system
 pH 5.6 NH₄AC-HAc -7.5×10⁻⁴g/ml AMH -0.375μg/ml HAuCl₄.

Table 1S Comparison of different analytical methods for B

Method	Principle	Linear range	Detection limit	Comments	Ref.
Fluorescence method	Base on the borate ion and alizarin red S using flow injection analysis of aqueous phase reaction	4 -40 μgml^{-1}	0.34 μgml^{-1}	Stability, suitable for the determination of ultra trace boron in environmental water samples, but the sensitivity is low	11
Quartz crystal resonator	Polymers with boron complexes, polymer film deposited on quartz crystal, the oscillation frequency is directly proportional to the change the concentration of boron .	0.3-80 $\mu\text{mol/L}$	0.3 $\mu\text{mol/L}$	complicated operation	44
Ion chromatography	Tetrafluoroborate ions change to boron	0.0667–1.0 M	----	Simple, stable. But the sensitivity was very low	29
voltammetry	Boron complexes with alizarin red S (ARS) complexes and the free ligands, adsorbed on the hanging mercury drop electrode	0–500 $\mu\text{g L}^{-1}$	15 $\mu\text{g L}^{-1}$	Stability, good selectivity, simple	12
ET-AAS	Determination of boron in shrimp by electrothermal atomic absorption spectrometry digestion and matrix (flux) separation approach for the	-	-	Stability, good selectivity, and applied to real life	9
ICP-AES	determination of boron in high-purity graphite powder using ICP-OES.	-	90 ng g ⁻¹	The content of boron in graphite powder can be detected in less than 1 ppm level	45
Spectrophotometry	In alkaline solution, lysine with and 1,2 - naphthoquinone	2.16–43.24 μgmL^{-1}	2 μgmL^{-1}	Fast, low cost, but the sensitivity is low	6

HPLC	<p>sulfonic acid and the -4- reaction of boron, charge transfer occurs</p> <p>Boron, at sub-ppm levels, in U₃O₈ powder and aluminum metal, was determined using complex formation and dynamically modified reversedphase high-performance liquid chromatography</p>	0.02-0.5µg	-	Simple, expensive instrument	47
SRET	<p>Rayleigh scattering resonance energy of nanogold transfer to the complex form by boric acid and AMH</p>	5-1000ng/mL		The method is simple, rapid, high sensitivity, stability, selectivity	This assay
SRET	<p>The Rayleigh scattering resonance energy of HAuCl₄ transfer to the complex form by boric acid and AMH</p>	5-600ng/mL		The method is simple, rapid, high sensitivity, stability, selectivity	This assay
Fluorescence method	<p>AMH with fluorescence, and after react with boric acid fluorescence quenching, gold nanoparticles can enhance the fluorescence quenching efficiency</p>	9-1000 ng/mL		The method is simple, rapid, high sensitivity	This assay
Fluorescence method	<p>AMH with fluorescence, and after react with boric acid fluorescence quenching, HAuCl₄ can enhance the fluorescence quenching efficiency</p>	9-500 ng/mL		The method is simple, rapid, high sensitivity	This assay

Table 2S Accuracy of the different boron systems

System	B concentration (ng/mL)	I	Average	RSD (%)
AMH-AuNPs	150	4293, 4087, 4155, 4400, 4044	4196	3.5
	180	3254, 3043, 3200, 3058, 3124	3156	2.9
AMH-HAuCl ₄	200	5623, 5824, 5577, 5702, 5500	5645	2.2
	500	3255, 2977, 2999, 3052, 3122	3081	3.6

Table 3S Effect of foreign substances

Coexistent substances	Tolerance ($\mu\text{mol/L}$)	Relative error(%)	Coexistent substances	Tolerance ($\mu\text{mol/L}$)	Relative error(%)
Mn ²⁺	400	0.36	F ⁻	400	-6.9
Cd ²⁺	400	5.1	IO ₃ ⁻	400	-8.7
Zn ²⁺	400	-1.14	SO ₄ ²⁻	400	0.5
Na ⁺	400	0.2	NO ₃ ⁻	400	5.8
Glucose	400	-7.5	ClO ₄ ⁻	400	2.1
Hg ²⁺	400	-3.9	Bi ³⁺	400	-0.3
Al ³⁺	400	0.4	SiO ₃ ²⁻	400	-4.6
Mannitol	400	6.7	H ₂ O ₂	400	-6.7
Glycerol	400	4.6	Glycol	400	-3.8
Salicylic acid	200	6.9	Mandelic acid	400	4.1
L-tyrosine	40	4.4	L-glutamic acid	200	-0.1

Table 4S Results for the determination of boron in water samples (n=5)

Sample	Single value (ng/mL)	Average (ng/mL)	B content (ng/mL)	Spiked B (ng/m L)	Found B (ng/mL)	Recovery (%)	RSD (%)
Sample 1	81.1, 85.3,	84.9	420	150	229.1	97.57	2.4
	90.6, 75.7, 92.0			200	324.1	96.8	2.7
Sample 2	58.7, 60.8,	59.0	300	150	199.8	95.6	1.7
	57.6, 44.3, 73.8			200	304.2	98.8	3.0
Sample 3	108.4, 103.3,	105.1	530	200	328.3	102.6	1.6
	92.0, 107.3, 114.4			400	461.7	99.7	4.1
Sample 4	23.7, 27.6,	24.9	120	200	301.4	109.6	2.6
	22.2, 23.8, 27.3			400	445.6	104.9	3.4
Sample 5	30.5, 23.1,	29.3	150	200	300.7	107.6	2.7
	30.4, 30.5, 31.8			400	446.3	103.9	4.1
Sample 6	56.4, 62.9,	57.9	290	200	310.7	100.9	3.7
	73.1, 47.1, 50.0			400	448.5	97.9	2.3